Bioorganic & Medicinal Chemistry Letters 21 (2011) 250–254

Contents lists available at ScienceDirect

Bioorganic & Medicinal Chemistry Letters

journal homepage: www.elsevier.com/locate/bmcl

Molecular modeling and UV–vis spectroscopic studies on the mechanism of action of reversed chloroquine (RCQ)

Vanessa A. Otelo [a], Antonio C. Sant'Ana [b,†], Dalva L. A. de Faria [b], Carla M. S. Menezes [a,‡,*]

[a] Programa de Pós-graduação em Fármaco e Medicamentos, Faculdade de Ciências Farmacêuticas, Universidade de São Paulo, Av. Prof. Lineu Prestes, 580 Bl. 13 sup., 05508-000 São Paulo, SP, Brazil
[b] Departamento de Química Fundamental, Instituto de Química, Universidade de São Paulo, Av. Prof. Lineu Prestes, 748 Bl. 4 inf., 05508-000 São Paulo, SP, Brazil

ARTICLE INFO

Article history:
Received 8 October 2010
Revised 1 November 2010
Accepted 2 November 2010
Available online 5 November 2010

Keywords:
Reversed chloroquine
Chloroquine
Heme
Antimalarial
Multiple ligand

ABSTRACT

Reversed chloroquine (**RCQ**) is a multiple ligand compound active against chloroquine-sensitive and resistant *falciparum* malaria. It is composed by a 4-aminoquinoline moiety (like that present in chloroquine (**CQ**)) joined to imipramine (**IMP**), a modulating agent that also showed intrinsic antiplasmodial activity against Brazilian *Plasmodium falciparum* isolates resistant to **CQ**. Molecular modeling and ultraviolet–visible spectroscopy (UV–vis) studies strongly suggest that the interaction between **RCQ** and heme is predominant through the quinoline moiety in a mechanism of action similar to that observed for **CQ**.

The paradigm of a multiple ligand on drug discovery emerged in the last decade to provide structural features to modulate multiple biological targets simultaneously in the same molecule.[1] The use of this new approach in the discovery of antimalarial drugs started with the so-called 'reversed chloroquine' (**RCQ**) (Fig. 1), a chloroquine-like compound[2] and has increased with the appointments of dihydropyrimidone[3] and acridone derivatives,[4] new analogs of reversed chloroquine,[5,6] and recently, modified 4-aminoquinolines and quinoline–acridine hybrids compounds.[7] These multiple ligand compounds have been able to modulate in vitro and in vivo chloroquine *Plasmodium falciparum* resistance and, at the same time, be active against sensitive strains. **RCQ**, its analogs and the acridone derivatives were supposed to show an antimalarial mechanism of action similar to chloroquine (**CQ**) (Fig. 1).[2–7] **CQ** is hypothesized to bind with heme, that corresponds to the toxic metabolic product resulting from the hemoglobin degradation by plasmodio.[8,9]

RCQ consists of a chloroquine-like moiety linked to the modulating agent imipramine (**IMP**) (Fig. 1) by both side-chains. It can thus be classified as a fused designed multiple ligand.[1] The quinoline moiety present in **RCQ** resembles the new antiplasmodial agent **AQ-13** (Fig. 1), a structural analog of **CQ** in which the side-chain has been simplified to a propyl group. This new 4-aminoquinoline compound has been considered as a candidate to antimalarial agent, with pharmacokinetic and toxicity properties similar to its prototype.[10] Imipramine and its desmethyl metabolite desipramine, two antidepressant drugs of the iminodibenzyl chemical class, were reported as in vitro promising modulating agents of **CQ** resistance in 1988.[11] Nevertheless, the clinical combination of desipramine and **CQ** was unsuccessful.[12] In a previous study using isolates of Brazilian *P. falciparum* resistant to **CQ**, we verified that both imipramine and desipramine showed intrinsic antiplasmodial activity in detriment to its modulating effect.[13] These data were further related to structural similarities between **CQ** and **IMP**,[14] features which allow us to hypothesize that **IMP** also interacts with heme.

Since **RCQ** is a chloroquine–imipramine hybrid molecule, its interaction with heme was investigated to simulate its probable mechanism of action. Molecular modeling and ultraviolet–visible (UV–vis) spectroscopy studies were used to address this issue.

The diprotonated form of **RCQ** (**RCQ.2H**$^+$), that of the *R*-diastereomer of chloroquine (**CQ.2H**$^+$), and the monoprotonated form of imipramine (**IMP.H**$^+$) were considered in the molecular modeling studies. The PM3 semiempirical method[15] was employed. The

* Corresponding author. Tel./fax: +55 21 25626478.
E-mail addresses: vaotelo@yahoo.com.br (V.A. Otelo), antonio.sant@ufjf.edu.br (A.C. Sant'Ana), dlafaria@iq.usp.br (D.L.A. de Faria), casmenezes@lassbio.icb.ufrj.br, casmenezes@yahoo.com (C.M.S. Menezes).
† Present address: Departamento de Química, Instituto de Ciências Exatas, Universidade Federal de Juiz de Fora, Rua José Lourenço Kelmer, s/n, 36036-330, Juiz de Fora, MG, Brazil.
‡ Present address: Laboratório de Avaliação e Síntese de Substâncias Bioativas (LASSBio, http://www.farmacia.ufrj.br/lassbio/), Faculdade de Farmácia, Universidade Federal do Rio de Janeiro, PO Box 68024, 21944-971 Rio de Janeiro, RJ, Brazil.

0960-894X/$ - see front matter © 2010 Elsevier Ltd. All rights reserved.
doi:10.1016/j.bmcl.2010.11.019

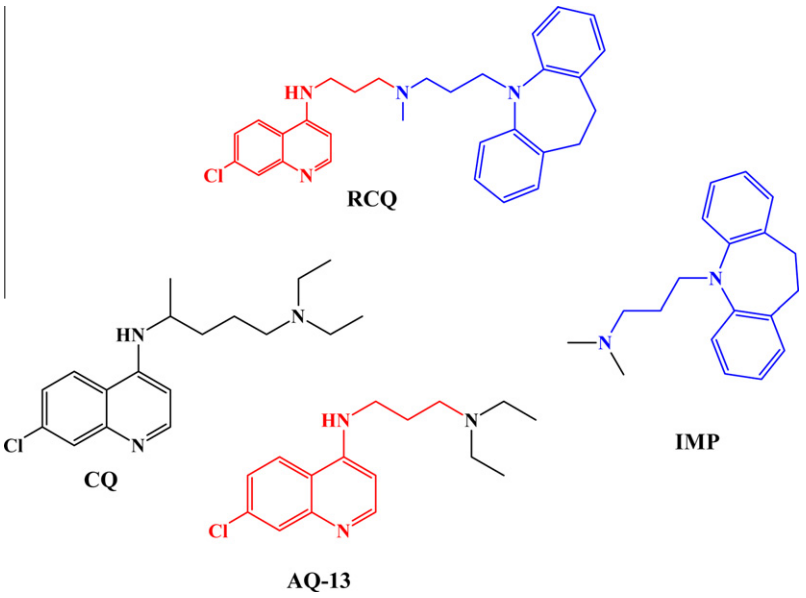

Figure 1. Chemical structures of reversed chloroquine (**RCQ**), chloroquine (**CQ**), the antimalarial candidate **AQ-13**, and imipramine (**IMP**).

molecular electrostatic potential maps show the quinoline and the right ring of the tricyclic moiety as the highest electronic density regions for **CQ.2H**$^+$ and **IMP.H**$^+$, respectively. The HOMO (Highest Occupied Molecular Orbital) distribution is also located on these electron-rich heterocyclic regions. The LUMO (Lowest Unoccupied Molecular Orbital) orbitals are concentrated around the charged nitrogen atom of the **IMP.H**$^+$ side-chain, whereas, for **CQ.2H**$^+$, they are located on the protonated quinoline ring. As a result of being a hybrid molecule, **RCQ.2H**$^+$ shows its highest electron density region and HOMO orbitals (Fig. 2B) located on the iminodibenzyl moiety while LUMO orbitals (Fig. 2C) are distributed on the protonated quinoline ring. These electronic features suggest that both moieties of **RCQ** may interact with the heme group since, in the case of **CQ**, such interaction is believed to occur through a co-facial π–π complex, as further discussed. Moreover, the HOMO and LUMO orbital distribution indicates the occurrence of a possible intramolecular interaction between the quinoline and iminodibenzyl moieties of **RCQ**.

Since **CQ** is reported to bind cofacially to unligated faces of heme (Fe(PPIX)) via π–π interaction, hematin (Fe(PPIX-OH)), one intermediate species in the heme detoxification process, was chosen to perform the docking study.[16] Analysis of the best fit, generated from Goldscore, indicate that **RCQ.2H**$^+$, **CQ.2H**$^+$, and **IMP.H** complex by a non-covalent mode with hematin (Fig. 3 illustrates the three complexes formed with the carboxylate specie of hematin). Chloroquine (**CQ.2H**$^+$) is planar to the iron–porphyrin system, with the quinoline moiety orientated toward the planar and electron-rich periphery region of hematin. In addition, the nitrogen aniline atom is orientated toward the iron atom, establishing an electron transfer interaction, while the side-chain interacts by attractive van der Waals forces with the porphyrin system. No salt bridge (dipole–dipole) interaction was observed between the protonated aliphatic nitrogen atom and the carboxylic groups, in spite of the neutral or carboxylate form of hematin. These molecular interactions corroborate previous theoretical and experimental reports. The formation of co-facial π–π complex between **CQ.2H**$^+$ and hematin was first reported by Fitch et al.[17] and have been supported by different experimental techniques such as nuclear magnetic resonance,[18] Mössbauer,[19] photoacoustic spectroscopy,[20] UV–vis spectrophotometry,[21,22] resonance Raman,[16] and theoretical methods.[23,24]

Imipramine (**IMP.H**$^+$) complexes similar to chloroquine (**CQ.2H**$^+$). The right benzene ring of the iminodibenzyl moiety is

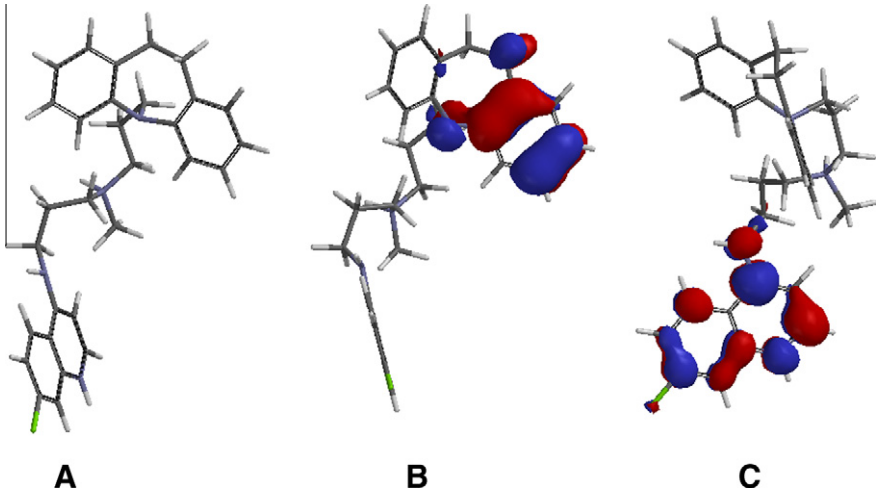

Figure 2. Minimum energy conformers of **RCQ.2H**$^+$ in the aqueous medium calculated using PM3 semiempirical method: (A) in the tube model; (B) HOMO and (C) LUMO orbital distributions at 0.032 eV. Atoms color: carbon (gray), nitrogen (blue), chlorine (green), and hydrogen (white).

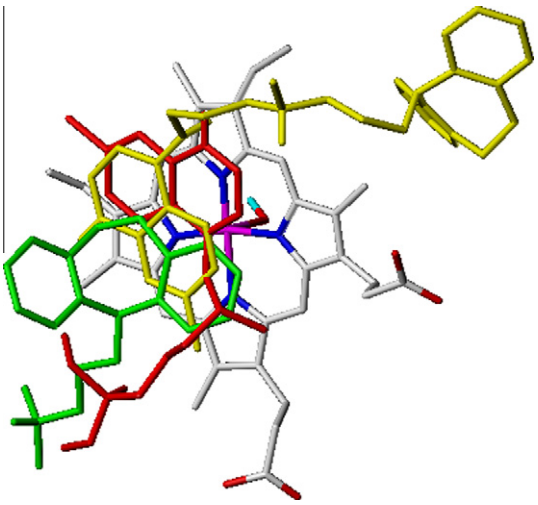

Figure 3. Structures of the complexes formed between hematin (carboxylate specie, C = white, N = blue, O = red, Fe = magenta, and H = cyan) and **RCQ.2H**$^+$ (yellow), **CQ.2H**$^+$ (red) and **IMP.H**$^+$ (green). The ligands are superimposed. Only polar hydrogen atoms are displayed.

oriented co-planar to the iron–porphyrin system, thus establishing π–π stacking interaction. In addition, van der Waals forces are present between the remaining heterocyclic moiety and the side-chain, which superimposes that of **CQ.2H**$^+$ (Fig. 3). Once more, no salt bridge interaction is observed between the protonated nitrogen atom (**IMP.H**$^+$) and the carboxylic oxygen atoms of hematin. Reversed chloroquine (**RCQ.2H**$^+$) docks preferentially by its quinoline moiety with the iron–porphyrin part of hematin. A coplanar orientation is observed between the quinoline moiety and hematin; furthermore, the **RCQ.2H**$^+$ quinoline moiety superimposes both the quinoline ring of **CQ.2H**$^+$ and the right ring of the iminodibenzyl moiety of **IMP.H**$^+$. Nevertheless, the quinoline orientation is slight different from that of chloroquine since the **RCQ** larger side-chain and the iminodibenzyl moiety also interact by van der Waals forces and orthogonal π-stacking with the periphery border of hematin. These results also suggest that steric properties could inhibit the approximation and binding of the quinoline moiety to hematin, explaining the observed loss of activity to some chloroquine reversed analogs.[5] Moreover, it is important to note that similar results were obtained when the hematin μ-oxo dimmer (Fe(III)PPIX μ-oxo dimer) was employed.

The UV–vis spectroscopy study considered a 1 hematin:2 compound stoichiometric ratio.[21,22] The spectra were obtained from aqueous solutions, prepared at pH 7.4 and 5.5 (resembling the food vacuole of plasmodio),[25]of the isolated compounds (**CQ**, **IMP**, and hematin), from binary mixtures (**CQ** + **IMP**; **CQ** + hematin, and **IMP** + hematin) and from the ternary mixture (**CQ** + **IMP** + hematin). In the later, hematin solution was added to a previously prepared solution containing **CQ** and **IMP**. For each mixture, to emphasize the chemical interaction effect, the UV–vis spectrum was compared to the spectrum generated mathematically by adding up the spectra from the isolated species.

The main advantages of using UV–vis spectroscopy in the study of molecular chemical interactions are that it allows the use of diluted solutions, compatible with biological or biochemical systems, and that such interactions affect the molecular energy levels causing shifts in band positions (bathochromic or hypsochromic shift), band broadening and/or changes in intensity (hyperchromism and hypochromism). With our previous knowledge of the electronic transitions responsible for the absorption bands, these changes can be used to track the nature of the chemical interaction and also its magnitude. Electrostatic interactions are much more difficult to detect since the effect on the energy levels is frequently negligible except when it affects molecular structure. Heme group presents two π–π* transitions corresponding to Soret or B bands around 380 nm and Q bands at near 550 nm. The Soret bands are assigned to the transition to the second excited state ($S_0 \rightarrow S_2$) while Q bands populate the first excited state ($S_0 \rightarrow S_1$),[26] with the transition moments strongly coupled through configuration interaction. In particular, Soret bands are sensitive to the chemical environment, and thus can be used to investigate interactions involving the heme group, including dimerization. It was recently shown that Soret has two bands: one at 385 nm, sensitive to the balance monomer–dimer, and another at 345 nm that independs of the interaction of the monomer–dimer.[27] The literature reports that dimerization causes a decrease in the 385 nm absorption band and the dimer is the predominant species in acidic solution.[28] In this study the Soret bands were used to analyze the interactions of the formed complexes.

Figure 4A and B shows the UV–vis spectra of aqueous buffer solutions, at pH 7.4 and 5.5, containing **CQ** or **IMP**, or both mixed, besides the sum of the spectrum of each isolated compound. Comparing the spectra of **CQ** and **IMP** isolated compounds at both pHs, it is clear that there is no significant effect of the pH on their spectra, an expected behavior since no additional protonation is expected at pH 5.5 due to the respective pK_a values (**CQ** pK_{a1} = 10.8, pK_{a2} = 8.4 and **IMP** pK_a = 10.2).[29] Other events, such as dimerization, are not reported for these compounds at the employed pH range. Hypochromism in the 200–250 nm absorption region is the only effect in the spectrum of the binary mixture that can be observed when compared with the sum of the spectra of each isolated compound. In this region, both compounds present π–π* transitions and the detected hypochromism may suggest that **CQ** and **IMP** interact through their heterocyclic moieties, reinforcing molecular modeling results. With the data available so far, it is not possible to conclude whether pH has or does not have an influence on the interaction, since the apparent less pronounced hypochromic effect at pH 5.5 may be an artifact due to the proximity of the spectral window edge.

From the heme aqueous solution (Fig. 5), the well known pH dependent monomer–dimer equilibrium[27] is responsible for the change in the Soret band shape when the two pHs are considered. As discussed above, dimerization causes a decrease in the intensity of the 385 nm Soret band[28] that makes clear that the dimer is the predominant species in acid solutions (Fig. 5C/D), while the monomer is the predominant species at pH 7.4 (Fig. 5A/B). The interaction of both compounds with heme is the main target of this UV–vis investigation. Binary and ternary mixtures were prepared and their spectra were compared with the sum of the isolated compounds spectra. Such a procedure highlights the eventual effect of a chemical interaction. A similar behavior, albeit less pronounced, is observed in the UV–vis spectra of the **IMP**-heme system (hypochromism of Soret bands and no significant changes in the band shapes, particularly in the case of heme) (Fig. 5B and D), again suggesting the existence of a weak interaction involving the **IMP** and heme aromatic rings. Concerning **CQ**, its interaction with heme was already investigated by UV–vis spectroscopy[21,22] and our results are in agreement with such works (Fig. 5A and C). The most remarkable feature in the **CQ**/heme spectrum is the change in the Soret band shape at both pHs, indicating that the compound is interfering with the heme monomer–dimer equilibrium. This reinforces the molecular modeling results, which indicated a relatively strong interaction via π-stacking. As expected, due to the simultaneous equilibrium present, the contribution of heme dimeric form to the spectrum of the **CQ**–heme mixture is more pronounced at pH 5.5, as shown by the strong absorption at 385 nm. From the UV–vis data reported here, it is clear that the **IMP**/heme interaction is much weaker than the **CQ**/heme one.

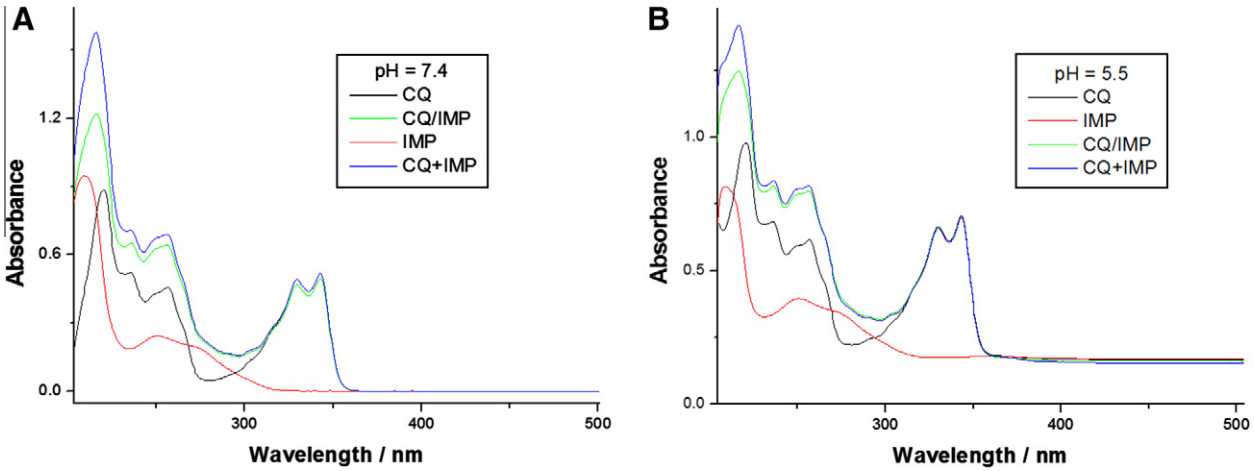

Figure 4. UV–vis spectra at pH 7.4 (A) and 5.5 (B) aqueous buffer solutions of chloroquine (**CQ**), imipramine (**IMP**), and a mixture of both solutions (**CQ/IMP**) and the result of adding up the spectrum of each isolated compound (**CQ** + **IMP**).

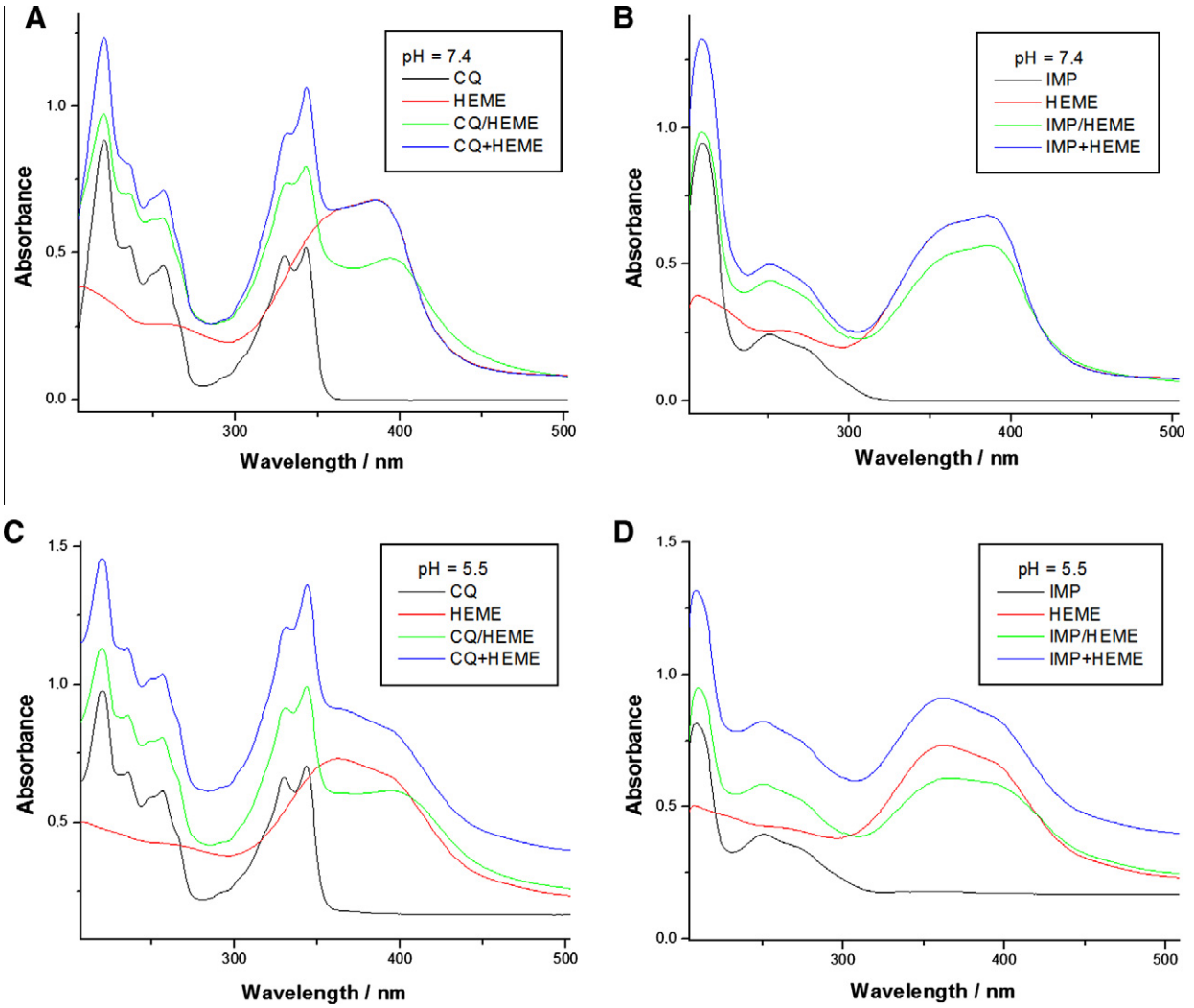

Figure 5. UV–vis spectra at pH 7.4 (A and B) and 5.5 (C and D) aqueous buffer solutions of **CQ**, **IMP**, heme, and the binary mixtures **CQ**/heme (A and C) and **IMP**/heme (B and D). The sum of **CQ** and heme spectra (**CQ** + heme) and of **IMP** and heme spectra (**IMP** + heme) was also included for comparison purposes.

The UV–vis spectra of the ternary mixtures (**CQ**/**IMP**/heme), at both pHs (Fig. 6A and B) show band positions and relative intensities similar to those obtained by the sum of the spectra of the binary **CQ**/heme and the isolated **IMP** solutions (**CQ**/heme + **IMP**), irrespective of the pH, but different from any other combination sum of the spectra of isolated + binary solutions. This fact

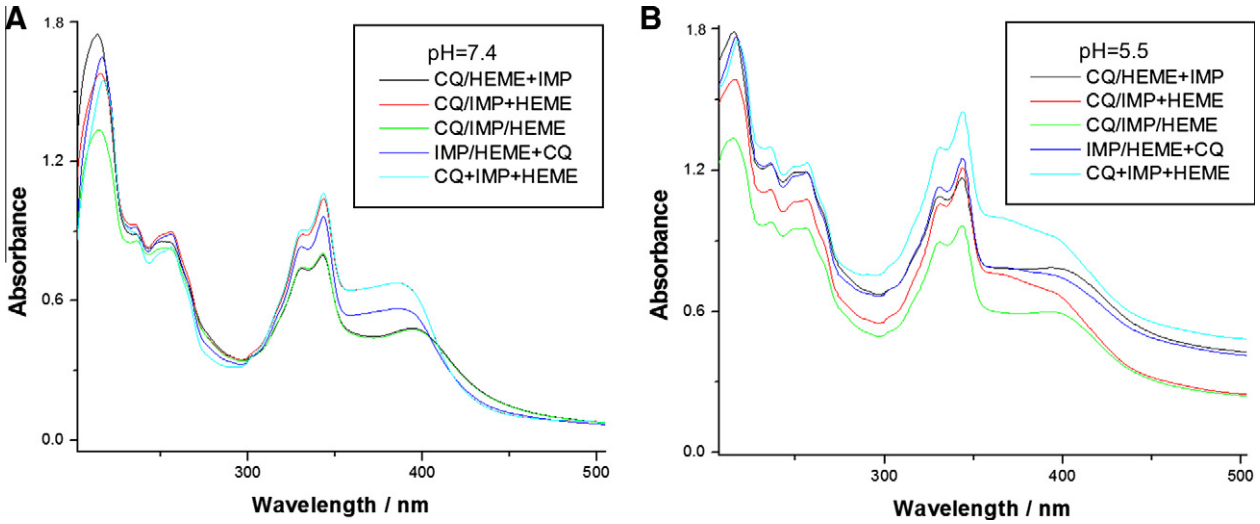

Figure 6. UV–vis spectra at pH 7.4 (A) and 5.5 (B) aqueous buffer solution of ternary mixture **CQ**/**IMP**/heme and the sums of the spectra of binary mixtures from **CQ**, **IMP**, and heme with the spectrum of the remaining isolated compound (**CQ**/IMP + heme, CQ/**heme** + **IMP** and **IMP**/heme + **CQ**), and the sum of the spectra of each isolated compound (**CQ** + **IMP** + heme), all original spectra obtained in aqueous buffer solution.

reinforces previous evidences that the **CQ**/heme interaction is stronger than the **IMP**/heme one, indicating that **CQ** is the preferred heme target. A similar interaction may occur with **RCQ**.

In conclusion, stereoelectronic features and docking complexes of **CQ**, **IMP** and **RCQ** combined with a careful UV–vis spectroscopy study indicated heme as the molecular target of action of **RCQ**, as previously supposed[2–7] and verified to occur biochemically,[6] by quinoline moiety interaction.

Acknowledgments

The authors are grateful to CAPES-ProDoc (00019 03-8) and CNPq for research grants and to Dr. Mauro A. La-Scalea (UNIFESP-Diadema) for donating the hemin chloride. C.M.S.M. is grateful to Professor Eliezer J. Barreiro (Chairman of LASSBio).

Supplementary data

Supplementary data associated with this article can be found, in the online version, at doi:10.1016/j.bmcl.2010.11.019.

References and notes

1. Morphy, R.; Rankovic, Z. *J. Med. Chem.* **2005**, *48*, 6523.
2. Burgess, S. J.; Selzer, A.; Kelly, J. X.; Smilkstein, M. J.; Riscoe, M. K.; Peyton, D. H. *J. Med. Chem.* **2006**, *49*, 5623.
3. October, N.; Watermeyer, N. D.; Yardley, V.; Egan, T. J.; Ncokazi, K.; Chibale, K. *ChemMedChem.* **2008**, *3*, 1649.
4. Kelly, J. X.; Smilkstein, M. J.; Brun, R.; Wittlin, S.; Cooper, R. A.; Lane, K. D.; Janowsky, A.; Johnson, R. A.; Dodean, R. A.; Winter, R.; Hinrichs, D. J.; Riscoe, M. K. *Nature* **2009**, *459*, 270.
5. Andrews, S.; Burgess, S. J.; Skaalrud, D.; Kelly, J. X.; Peyton, D. H. *J. Med. Chem.* **2010**, *53*, 916.
6. Burgess, S. J.; Kelly, J. X.; Shomloo, S.; Wittlin, S.; Brun, R.; Liebmann, K.; Peyton, D. H. *J. Med. Chem.* **2010**, *53*, 6477.
7. Kumar, S.; Srivastava, K.; Raja-Kumar, S.; Puri, S. K.; Chauhan, P. M. S. *Bioorg. Med. Chem. Lett.* **2010**. doi:10.1016/j.bmcl.2010.09.107.
8. Kumar, S.; Guha, M.; Choubey, V.; Maity, P.; Bandyopadhayay, U. *Life Sci.* **2007**, *80*, 813.
9. Nilesa, J. C.; DeRisi, J. L.; Marletta, M. A. *Proc. Natl. Acad. Sci. U.S.A.* **2009**, *106*, 13266.
10. Mzayek, F.; Deng, H.; Mather, F. J.; Wasilevich, E. C.; Liu, H.; Hadi, C. M.; Chansolme, D. H.; Murphy, H. A.; Melek, B. H.; Tenaglia, A. N.; Mushatt, D. M.; Dreisbach, A. W.; Lertora, J. J. L.; Krogstad, D. J. *PLoS Clin. Trial.* **2007**, *2*, e6.
11. Bitonti, A. J.; Sjoerdsma, A.; McCann, P. P.; Kyle, D. E.; Oduola, A. M.; Rossan, R. N.; Milhous, W. K.; Davidson, D. E. *Science* **1988**, *242*, 1301.
12. Warsame, M.; Wernsdorfer, W. H.; Björkman, A. *Trans. R. Soc. Trop. Med. Hyg.* **1992**, *86*, 235.
13. Menezes, C. M. S.; Kirchgatter, K.; Di Santi, S. M. F.; Savalli, C.; Monteiro, F. G.; Paula, G. A.; Ferreira, E. I. *Trans. R. Soc. Trop. Med. Hyg.* **1997**, *91*, 697.
14. Menezes, C. M. S.; Ferreira, E. I. *Drugs Des. Rev. Online* **2005**, *2*, 409.
15. Stewart, J. J. P. *J. Comput. Aided Mol. Des.* **1990**, *4*, 1.
16. Webster, G. T.; McNaughton, D.; Wood, B. R. *J. Phys. Chem.* **2009**, *113*, 6910.
17. Fitch, C. D.; Chevli, R.; Banyal, H. S.; Phillips, G.; Pfaller, M. A.; Krogstad, D. J. *Antimicrob. Agents Chemother.* **1982**, *21*, 819.
18. Leed, A.; DuBay, K.; Ursos, L. M.; Sears, D.; de Dios, A. C.; Roepe, P. D. *Biochemistry* **2002**, *41*, 10245.
19. Adams, P. A.; Egan, T. J.; Ross, D. C.; Silver, J.; Marsh, P. J. *Biochem. J.* **1996**, *318*, 25.
20. Balasubramanian, D.; Rao, C. M.; Panijpan, B. *Science* **1984**, *223*, 828.
21. Egan, T. J. *J. Inorg. Biochem.* **2006**, *100*, 916.
22. Kalkanidis, M.; Klonis, N.; Tilley, L.; Deady, L. W. *Biochem. Pharmacol.* **2002**, *63*, 833.
23. Portela, C.; Afonso, C. M. M.; Pinto, M. M. P.; Ramos, M. J. *FEBS Lett.* **2003**, *27435*, 217.
24. Portela, C.; Afonso, C. M. M.; Pinto, M. M. M.; Ramos, M. J. *J. Comput. Aided Mol. Des.* **2003**, *17*, 583.
25. Yayon, A.; Cabantchik, Z. I.; Ginsburg, H. *EMBO J.* **1984**, *11*, 2695.
26. Anderson, H. L. *Chem. Commun.* **1999**, *23*, 2323.
27. de Villiers, K. A.; Kaschula, C. H.; Egan, T. J.; Marques, H. M. *J. Biol. Inorg. Chem.* **2007**, *12*, 101.
28. Wood, B. R.; Langford, S. J.; Cooke, B. M.; Lim, J.; Glenister, F. K.; Duriska, M.; Unthank, J. T.; McNaughton, D. *J. Am. Chem. Soc.* **2004**, *126*, 9233.
29. Clarke, E. G. C. *Isolation and Identification of Drugs: In Pharmaceutical, Body fluids and Postmortem Material*, 2nd ed.; Pharmaceutical Press: London, 1986.